

Wide-Area GNSS Spoofing and Jamming Detection Using AIS-Derived Spatiotemporal Integrity Monitoring

Sanghyeon Park¹, DeukJae Cho², Pyo-Woong Son¹

¹ Department of Electronics Engineering, Chungbuk National University, Cheongju, 28644, Republic of Korea

² Maritime Digital Transformation Research Center, Korea Research Institute of Ships and Ocean Engineering, 34103, Daejeon, Republic of Korea

Correspondence

Pyo-Woong Son. E-mail: pwson@cbnu.ac.kr

Abstract

Global Navigation Satellite System (GNSS) spoofing and jamming threaten maritime navigation by corrupting positions from Automatic Identification System (AIS) transponders. Crucially, raw AIS messages contain communication-layer defects—duplicated MMSIs, timestamp errors, stale retransmissions and multi-station rebroadcast delays—that mimic spoofing or jamming. Thus, AIS positions are unreliable without pre-filtering. We propose a three-stage AIS-based framework that (1) uses rule-based diagnostics to discard communication faults, (2) applies an interacting multiple model filter and transmission-interval analysis to extract kinematic-consistency and continuity anomalies, and (3) spatiotemporal DBSCAN to group anomalies by multi-vessel coherence and temporal persistence and classify them as sensor faults, spoofing or jamming. Tested on approximately 966 million AIS messages from Korean coastal waters, the framework detected 17 spoofing and 343 jamming clusters and reduced false alarms by 98.6 % relative to naive clustering. These results show, after rigorous pre-filtering, AIS data can enable wide-area GNSS interference detection without dedicated sensors.

Keywords

AIS, Anomaly detection, GNSS interference, Kalman filter, Spatiotemporal DBSCAN

1. INTRODUCTION

Maritime navigation and surveillance systems rely critically on the integrity of Positioning, Navigation, and Timing (PNT) information (International Civil Aviation Organization [ICAO], International Maritime Organization [IMO], & International Telecommunication Union [ITU], 2025). The Automatic Identification System (AIS), mandated by the International Maritime Organization for safety-of-life-at-sea (SOLAS) vessels, has become a cornerstone of maritime situational awareness by continuously broadcasting vessel position, speed, and course (IMO, 2002). These AIS reports support collision avoidance, vessel traffic services, and large-scale maritime monitoring. However, because AIS position information is predominantly derived from unencrypted Global Navigation Satellite System (GNSS) signals, it is inherently vulnerable to both intentional and unintentional disruptions (International Association of Independent Tanker Owners [INTERTANKO], 2019).

In recent years, multiple incidents have demonstrated the operational impact of GNSS degradation in maritime environments. Large-scale GNSS jamming and spoofing events have been documented across the Baltic Sea, Eastern Mediterranean, and Black Sea regions, affecting both aviation and maritime operations (Felux et al., 2024; European Union Aviation Safety Agency [EASA], 2023). In 2023–2024, spoofing incidents displaced over 100 vessels simultaneously to false airport positions in the Eastern Mediterranean (Lo et al., 2025), while AIS manipulation for sanctions evasion has been increasingly reported (Androjna et al., 2024). GNSS spoofing can distort vessel trajectories by manipulating position solutions, while GNSS jamming can completely disrupt navigation by preventing receivers from obtaining valid fixes (IMO, 2021). Such events pose serious risks to maritime safety, particularly in congested coastal waters and strategic sea lanes. Consequently, there is growing interest in AIS-based methods for detecting GNSS interference at regional scales, where dedicated GNSS monitoring infrastructure may be sparse or unavailable (International Association of Marine Aids to Navigation and Lighthouse Authorities [IALA], 2016).

A substantial body of research has explored AIS-based anomaly detection using data-driven trajectory analysis, physical kinematic modeling, or hybrid approaches. A comprehensive review by Wolsing et al. (2022) surveyed 44 research articles on AIS track anomaly detection, identifying ten groups of detection methods ranging from clustering to deep learning. Data-driven methods identify statistical deviations from historical traffic patterns, while kinematic models evaluate whether reported vessel motion violates physical constraints. Although these approaches can detect anomalous vessel behavior, they face two fundamental challenges when applied to GNSS interference monitoring. First, AIS data are affected by a wide range of non-GNSS-related irregularities, including communication-layer faults and onboard sensor issues, which can easily be misclassified as interference-induced anomalies (El Mekkaoui et al., 2022; Harati-Mokhtari et al., 2007). Second, many existing methods analyze vessels independently and therefore fail to capture multi-vessel coherence, a defining characteristic of wide-area GNSS spoofing and jamming (Ferreira et al., 2022). Statistical frameworks for detecting malicious AIS spoofing have been proposed (d’Afflisio et al., 2021), yet these approaches still lack explicit mechanisms to distinguish communication-layer artifacts from genuine interference.

AIS communication-integrity artifacts represent a particularly significant source of false alarms. The importance of data integrity assessment in maritime anomaly detection has been emphasized by Iphar et al. (2020), who showed that AIS quality issues can substantially degrade detection reliability. Concurrent reuse of Maritime Mobile Service Identity (MMSI) identifiers by multiple vessels can create artificial position jumps when tracks are reconstructed, even though each vessel individually follows a physically plausible trajectory (Zhao et al., 2018). Similarly, timestamp-delayed retransmission of AIS messages—caused by buffering or synchronization issues—can generate apparent backward motion or duplicated positions (ITU, 2014). These artifacts originate from the AIS communication chain rather than from GNSS degradation, yet they are frequently treated as generic anomalies in existing detection frameworks. In addition to communication faults, vessel-specific sensor-integrity issues further complicate AIS-based analysis. Extreme position or velocity deviations may arise from degraded GNSS receivers, multipath effects, or transient measurement glitches (IALA, 2016). Such anomalies can produce kinematic inconsistencies comparable in magnitude to those induced by spoofing, despite being confined to a single vessel. Without explicit mechanisms to distinguish persistent or transient sensor-related irregularities from coordinated multi-vessel behavior, kinematic anomaly detectors alone cannot reliably infer the presence of external GNSS interference (Ferreira et al., 2022).

Another critical limitation of prior studies is their treatment of GNSS jamming. Unlike spoofing, which manifests as distorted trajectories, jamming often results in the absence of valid position reports altogether (INTERTANKO, 2019). During such outages, AIS messages may cease or be transmitted at irregular intervals, rendering conventional trajectory-based detection ineffective (ITU, 2014). Robust detection of jamming therefore requires explicit analysis of transmission continuity in addition to kinematic behavior (Last et al., 2014).

To address these challenges, this paper proposes a unified AIS-based framework for wide-area GNSS interference detection that explicitly separates communication faults, sensor-integrity artifacts, and

genuine GNSS interference. Communication-integrity artifacts—including concurrent MMSI duplication and timestamp-delayed AIS message rebroadcast—are first identified and removed through rule-based diagnostics. All remaining anomalies, including extreme position and velocity deviations, are preserved and forwarded to a spatiotemporal clustering stage.

Using ST-DBSCAN, the framework classifies anomalies according to persistence and multi-vessel coherence. Vessel-specific anomalies are categorized as persistent or transient sensor-integrity artifacts, reflecting long-term degradation or short-lived measurement irregularities, respectively. In contrast, anomalies shared by multiple vessels within common spatial and temporal bounds are classified as GNSS spoofing or GNSS jamming events, depending on whether they manifest as coordinated kinematic distortion or concurrent reporting outages. This hierarchical design enables robust discrimination between AIS communication artifacts, vessel-level sensor irregularities, and region-level GNSS interference within a single processing pipeline.

The remainder of this paper is organized as follows. Section 2 reviews existing AIS-based anomaly detection studies and identifies their limitations in handling communication faults, sensor-integrity issues, and multi-vessel coherence. Section 3 presents the proposed framework in detail. Section 4 describes the dataset and experimental setup. Section 5 analyzes representative case studies demonstrating the classification of communication-integrity artifacts, sensor-integrity artifacts, and spatiotemporally shared GNSS spoofing and jamming events. Section 6 discusses practical implications and limitations, and Section 7 concludes the paper.

2. RELATED WORKS

2.1 Communication Integrity and AIS Data Quality Issues

Beyond trajectory anomalies, AIS communication itself introduces multiple data-quality issues that can mimic GNSS interference and inflate false alarm rates if not explicitly addressed (El Mekkaoui et al., 2022). A well-documented example is MMSI duplication, where distinct vessels broadcast the same identifier due to configuration errors or reused transponders (Harati-Mokhtari et al., 2007). Shore-station or receiver time-synchronization errors can also produce contradictory multi-position reports for a single MMSI (Fukuda et al., 2024). Meanwhile, oscillatory jitter or retransmission of stale data commonly results in physically inconsistent trajectories that resemble spoofing-induced distortions. Additionally, infrastructure-induced inconsistencies, such as multi-receiver rebroadcast delays, may generate position scattering that confounds naive anomaly detectors.

These communication-layer artifacts originate from the AIS transmission chain rather than from navigation sensor degradation. Nevertheless, they are frequently misclassified as GNSS anomalies in existing AIS-based detection studies, underscoring the necessity of integrating communication-integrity diagnostics into AIS-based monitoring frameworks. Without such diagnostics, anomaly detection results cannot be reliably interpreted or operationalized.

2.2 AIS Data-Driven Anomaly Detection

A large body of AIS anomaly detection research has relied on data-driven approaches, where normal vessel behavior is modeled from historical AIS trajectories and deviations are identified statistically. Classical clustering methods such as DBSCAN have been used to distinguish between stationary and moving clusters and to detect outliers that deviate from typical spatial patterns (Ferreira et al., 2022; Goodarzi & Shaabani, 2019; Han et al., 2021; Newaliya & Singh, 2024; Rong et al., 2020).

Complementary approaches estimate expected trajectories through kinematic interpolation or prediction models and classify large residuals as anomalies (Guo et al., 2021). More recently, deep-learning-based frameworks—ranging from probabilistic neural representations to convolutional architectures—have demonstrated improved capability in capturing complex motion dependencies and detecting abnormal behavior in data-rich environments (Liang et al., 2024; Lv et al., 2025; Nguyen et al., 2022).

Despite these advancements, data-driven methods remain fundamentally constrained by the distributions on which they are trained. Their performance deteriorates when exposed to rare, emerging, or region-

specific motion patterns that differ from the training set. Moreover, the anomaly decisions produced by deep-learning models often lack interpretability, providing little insight into whether the irregularity originates from GNSS degradation, vessel-specific sensor-integrity issues, or AIS communication faults. Finally, most data-driven studies focus exclusively on single-vessel trajectories, leaving them unable to detect collective anomalies, which are a defining signature of wide-area GNSS interference.

2.3 Dynamic-State and Kinematic Modeling Approaches

To improve interpretability and incorporate physical constraints, several studies have applied dynamic-state estimation and kinematic modeling to AIS anomaly detection. Early work demonstrated the use of Extended Kalman Filters (EKF) to track vessel trajectories and flag physically implausible measurements (Liu et al., 2019; Mai Thi et al., 2024; Siegert et al., 2016). More advanced studies introduced the Interacting Multiple Model (IMM) filter, which combines Constant Velocity (CV) and Constant Turn Rate and Velocity (CTRV) models to handle both straight-line and maneuvering behavior without requiring training data (Genovese, 2001; Tian et al., 2025; Yang et al., 2022).

Kinematic filtering provides clear interpretability, since detected anomalies correspond directly to violations of motion feasibility such as unrealistic acceleration or discontinuous headings. However, these methods still operate primarily on individual vessel trajectories, making them unsuitable for detecting region-level anomalies that affect multiple vessels simultaneously. Moreover, kinematic approaches alone cannot differentiate external GNSS distortion from vessel-specific sensor-integrity issues or AIS communication-layer artifacts, including MMSI misuse or delayed retransmission. Most critically, they cannot be applied when AIS position reports cease entirely during GNSS jamming, which eliminates the positional data required for kinematic evaluation.

2.4 Spatiotemporal Clustering for Maritime Anomalies

Recognizing that wide-area GNSS interference often manifests as coordinated anomalies across multiple vessels, recent studies have adopted spatiotemporal clustering techniques—particularly ST-DBSCAN—to identify groups of irregular observations (Birant & Kut, 2007). ST-DBSCAN extends DBSCAN by incorporating a temporal radius in addition to a spatial radius, enabling detection of dense anomaly clusters that persist across space and time. This approach has been used to reveal abnormal regional behaviors, including both localized disruptions and broader traffic inconsistencies (Olesen et al., 2023). However, prior applications of ST-DBSCAN typically rely on raw AIS observations or simple trajectory deviations as inputs, without incorporating domain-specific validation of kinematic feasibility or communication integrity. As a result, spatiotemporal clusters can arise from fundamentally different sources—including GNSS spoofing, MMSI duplication, multi-station synchronization errors, or sensor-integrity artifacts—yet appear indistinguishable in cluster outputs. Without upstream diagnostics or multi-layer validation, spatiotemporal clustering alone cannot reliably separate true GNSS interference from AIS system artifacts.

3. METHODOLOGY

3.1 Overview of the Unified Processing Pipeline

This study proposes a unified AIS-based processing pipeline designed to reliably distinguish wide-area GNSS interference from communication-layer artifacts and vessel-specific sensor irregularities. The overall architecture, illustrated in Figure 1, follows a hierarchical structure in which anomaly sources are progressively separated based on their physical origin and spatiotemporal characteristics.

The pipeline consists of three conceptually distinct stages. First, communication-integrity diagnostics are applied to AIS messages to identify and remove artifacts arising from identifier misuse or transmission irregularities. Second, potential anomaly cues are generated from AIS trajectories and transmission records without performing any premature classification or removal. These cues capture heterogeneous

manifestations of GNSS-related irregularities, including kinematic inconsistencies and reporting outages. Finally, all preserved anomaly cues are jointly analyzed through spatiotemporal clustering to differentiate vessel-specific sensor-integrity artifacts from spatiotemporally shared GNSS spoofing and jamming events.

A key design principle of the proposed framework is that only communication-integrity artifacts are removed prior to clustering, while all other anomalies are retained and classified based on persistence and multi-vessel coherence. This design ensures that sensor-related irregularities are not misinterpreted as GNSS interference and that wide-area events are identified through collective behavior rather than isolated deviations.

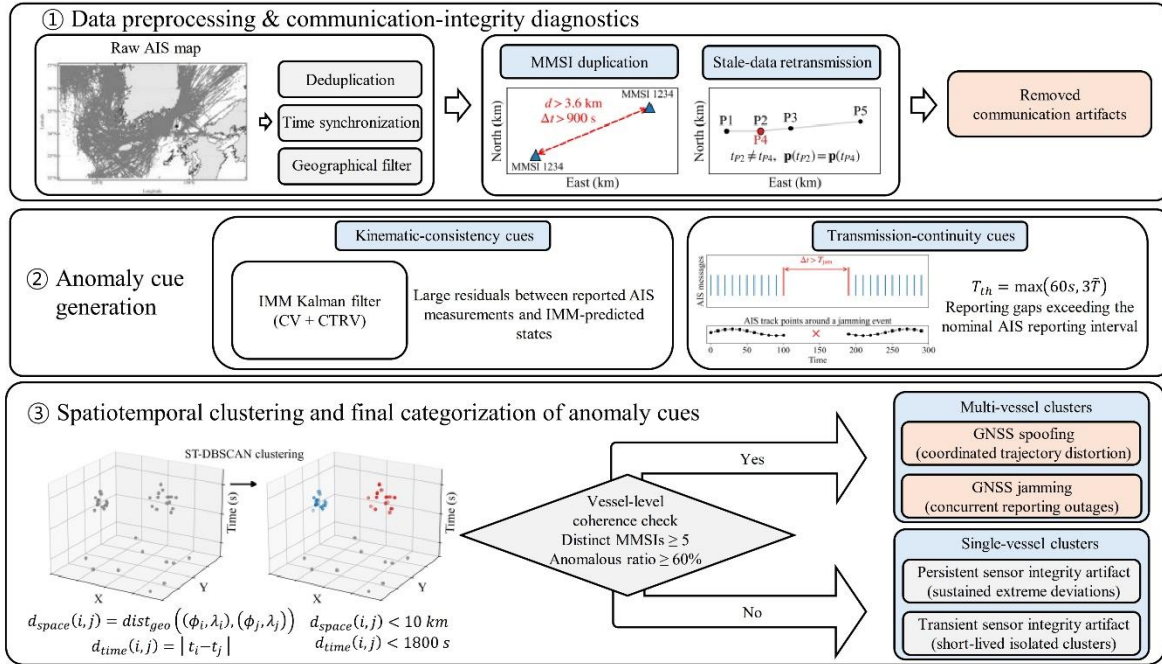


FIGURE 1 Flowchart of the proposed hierarchical processing pipeline for AIS-based GNSS interference detection, comprising communication-integrity diagnostics, anomaly cue generation, and spatiotemporal clustering with final categorization

3.2 Communication-Integrity Diagnostics

Certain AIS anomalies originate from communication-layer faults rather than from navigation sensor degradation or GNSS interference. To prevent such artifacts from inflating false alarm rates, two representative communication-integrity issues are explicitly diagnosed and removed at an early stage: concurrent MMSI duplication and timestamp-delayed retransmission of AIS messages.

MMSI duplication occurs when multiple vessels broadcast the same identifier within overlapping time intervals while being separated by distances exceeding feasible vessel motion constraints. This artifact produces artificial position jumps in reconstructed trajectories, despite each vessel individually exhibiting physically plausible dynamics (Goodarzi & Shaabani, 2019; Olesen et al., 2023; Zhang & Li, 2022). MMSI duplication is identified using spatial and temporal consistency checks, as summarized in Algorithm 1.

ALGORITHM 1 MMSI duplication verification process

Input: Call (clusters from 1st analysis)

Params: $\{\epsilon_{space}, \epsilon_{time}, \epsilon_{speed}, \epsilon_{heading}, duration\}$

1: **Step 1: Related Cluster Identification**

2: for each pair (C_i, C_j) in Call do

3: if $\exists m$ (MMSI) such that $m \in C_i$ and $m \in C_j$ and $TimeRange(C_i) \cap TimeRange(C_j) \neq \emptyset$ then

4: Define (C_i, C_j) as a related pair

5: end if

6: end for

7: Group related clusters into components G_1, G_2, \dots, G_n

8: **Step 2: Sub-track Extraction and Validation**

9: for each group G do

10: NormalTracks $\leftarrow \emptyset$

11: for each MMSI $\in G$ do

12: Apply DBSCAN with spatial, temporal, velocity, and heading constraints

13: Keep sub-tracks with duration ≥ 10 min

14: for each sub-track T do

15: Apply IMM-Kalman filter to validate normality

16: if $isNormal(T) = True$ then

17: Add T to NormalTracks

18: end if

19: end for

20: end for

21: **Step 3: Group-level Decision Rule for group G**

22: if $|NormalTracks| \geq 2$ then

23: Label group G as MMSI Duplication and remove from GNSS anomaly candidates

24: else if $|NormalTracks| = 1$ then

25: Label the single normal sub-track as True Track

26: Reclassify the remaining duplicated tracks of this MMSI as MMSI Duplication

27: else

28: Retain all tracks in G as GNSS anomaly candidates

29: end if

30: end for

31: **Step 4: Intra-cluster Revalidation**

32: for each cluster C classified as “Single vessel cluster” do

33: Repeat Steps 2–3 within C

34: if ≥ 2 normal overlapping sub-tracks exist then

35: Label C as MMSI Duplication

36: end if

37: end for

Output: Updated cluster labels (MMSI Duplication / Anomaly Candidate)

Timestamp-delayed retransmission arises when previously transmitted AIS navigation tuples are rebroadcast with updated timestamps due to buffering, synchronization, or relay errors. Such retransmissions generate duplicated positions or backward motion artifacts that resemble trajectory distortion. Algorithm 2 verifies stale-data retransmission by detecting repeated navigation tuples with inconsistent temporal ordering.

ALGORITHM 2 stale-data retransmission verification process

Input: AIS data $\{(Lat_t, Lon_t, SOG_t, COG_t, t)\}$ for a single MMSI

1: **Step 1: Initialize lookup table**

2: Initialize an empty map D (D: key = (Lat, Lon, SOG, COG), value = latest timestamp)

3: **Step 2: Scan AIS sequence and detect repeated tuples**

4: for each record at time t in chronological order do

5: $key_t \leftarrow (Lat_t, Lon_t, SOG_t, COG_t)$

6: if $key_t \in D$ and $D[key_t] \neq t$ then

7: Classify current point as Stale-Data Retransmission

8: Update $D[key_t] \leftarrow t$

9: else

10: Insert key_t into D with timestamp t

11: end if

12: end for

Output: Updated data labels (Stale-Data Retransmission / Anomaly Candidate)

Because both artifacts originate from the AIS communication chain rather than from navigation or GNSS performance, they are removed from further analysis once identified. No kinematic or sensor-related anomalies are removed at this stage, ensuring that subsequent classification is based solely on navigation-relevant information.

3.3 Anomaly Cue Generation

After communication-integrity diagnostics, the remaining AIS data may still contain irregularities originating from navigation sensor degradation or external GNSS interference. Rather than attempting to classify or remove such anomalies in isolation, the proposed framework extracts anomaly cues that are preserved for subsequent spatiotemporal clustering. Two complementary types of anomaly cues are generated: kinematic-consistency cues derived from vessel motion and transmission-continuity cues derived from AIS reporting behavior.

3.3.1 Kinematic Anomaly Cues via IMM

For AIS trajectories with valid position reports, kinematic-consistency cues are extracted using an Interacting Multiple Model (IMM) filter combining Constant Velocity (CV) and Constant Turn Rate and Velocity (CTRV) motion models as depicted in Figure 2. The IMM filter estimates vessel state while accommodating both straight-line and maneuvering behavior without requiring training data.

The vessel state vector at time step k is defined as

$$x_k = [p_x, p_y, v, \psi, \dot{\psi}]^T \quad (1)$$

where p_x, p_y , represent the planar position (m), v is the speed (m/s), ψ the heading angle (rad), and $\dot{\psi}$ the yaw rate (rad/s).

Each motion model propagates the state through its dynamic equations with corresponding process noise covariance. After prediction, the IMM fuses the individual model estimates using normalized mode probabilities:

$$x_k = \sum_i \mu_{i,k} x_{i,k}, P_k = \sum_i \mu_{i,k} [P_{i,k} + (x_{i,k} - x_k)(x_{i,k} - x_k)^T] \quad (2)$$

where $\mu_{i,k}$ is the normalized probability of model i, and P_k is the fused covariance matrix.

Large residuals between reported AIS measurements and IMM-predicted states indicate violations of physical motion feasibility, such as abrupt position jumps, unrealistic accelerations, or discontinuous velocity changes. These residuals are recorded as kinematic anomaly cues. Importantly, such cues may arise from either vessel-specific sensor-integrity issues or external GNSS distortion, and are therefore not interpreted independently at this stage.

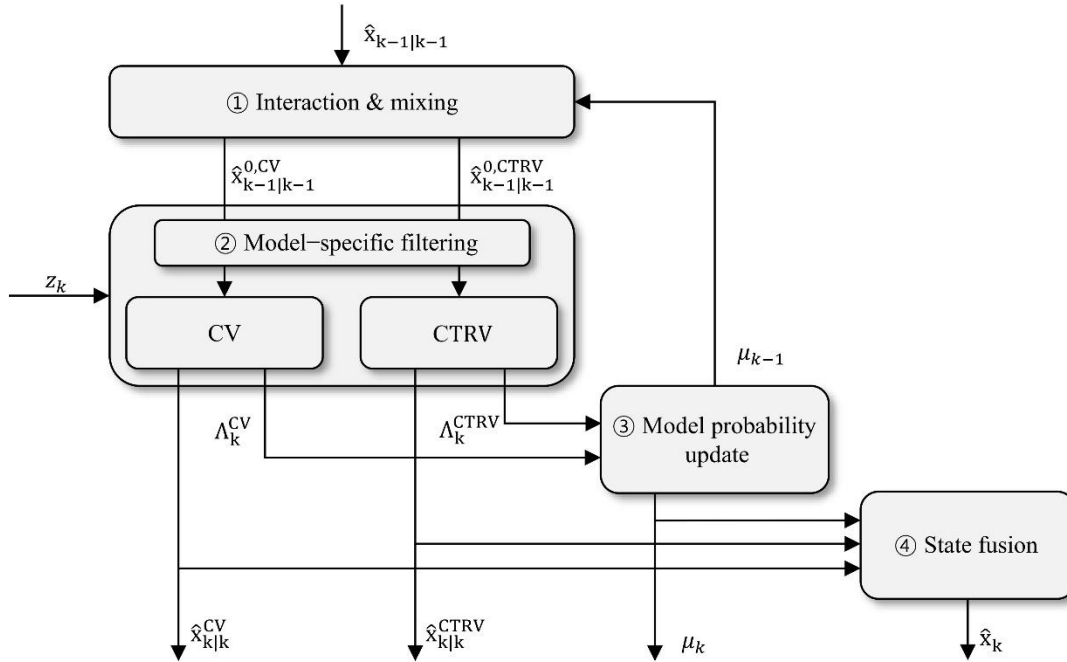


FIGURE 2 Structure of the Interacting Multiple Model (IMM) filter combining Constant Velocity (CV) and Constant Turn Rate and Velocity (CTRV) motion models for kinematic-consistency screening of AIS trajectories

3.3.2 Transmission-Interval Anomaly Cues for Jamming

AIS transmission-continuity cues are extracted by analyzing inter-message intervals for each vessel. When a GNSS receiver fails to produce a valid position solution, AIS position reports may cease or be transmitted at irregular intervals. Reporting gaps exceeding the nominal AIS Class-A interval are therefore treated as outage-related anomaly cues. To capture this effect, the framework computes the vessel-specific median reporting interval \tilde{T} during normal navigation (SOG > 1 m/s) and defines a jamming-suspicion threshold:

$$T_{th} = \max(60s, 3\tilde{T}) \quad (3)$$

where the 60s minimum ensures that jamming events exceed typical AIS Class A/B reporting behavior.

An interval is marked as a jamming anomaly candidate if:

$$T_k > T_{th}. \quad (4)$$

These transmission-interval anomalies are preserved without classification, as isolated outages may reflect vessel-specific receiver issues, whereas simultaneous outages across multiple vessels may indicate wide-area GNSS jamming. Final interpretation is deferred to the clustering stage, where multi-vessel coherence can be assessed.

3.4 Spatiotemporal Clustering and Final Categorization of Anomaly Cues

In the fourth stage of the unified processing pipeline defined in Section 3.1, all preserved anomaly cues are embedded into a joint spatiotemporal space and analyzed using the ST-DBSCAN algorithm. By extending DBSCAN with temporal constraints, ST-DBSCAN enables systematic grouping of anomalies that are coherent in both space and time, thereby providing the basis for final anomaly categorization. For each anomaly candidate i , the spatial and temporal separations from another candidate j are defined as

$$d_{\text{space}}(i, j) = \text{dist}_{\text{geo}}((\phi_i, \lambda_i), (\phi_j, \lambda_j)), d_{\text{time}}(i, j) = |t_i - t_j|, \quad (5)$$

where $\text{dist}_{\text{geo}}(\cdot)$ denotes the great-circle (geodesic) distance on the WGS-84 ellipsoid, and $d_{\text{time}}(i, j)$ is the absolute time difference between the two events. A pair of anomalies i and j are regarded as neighbors when:

$$d_{\text{space}}(i, j) < \varepsilon_s, d_{\text{time}}(i, j) < \varepsilon_t, \quad (6)$$

where $\varepsilon_s = 10$ km and $\varepsilon_t = 1800$ s were selected based on typical vessel separation scales and temporal coherence observed in coastal waters.

Based on these definitions, ST-DBSCAN performs anomaly grouping and final categorization through the following steps:

- (1) Anomalies are first grouped according to spatiotemporal proximity, forming candidate clusters that may involve either single or multiple vessels.
- (2) Cluster composition is then evaluated to distinguish isolated vessel-level anomalies from multi-vessel structures sharing common spatial and temporal bounds.
- (3) The temporal persistence of each cluster is examined to differentiate sustained irregularities from short-lived events.

Through this process, single-vessel clusters exhibiting sustained extreme deviations are classified as persistent sensor-integrity artifacts, whereas short-lived isolated clusters are classified as transient sensor-integrity artifacts. In contrast, clusters involving multiple vessels are interpreted as manifestations of external GNSS interference. When such multi-vessel clusters primarily exhibit coordinated trajectory distortion, they are classified as GNSS spoofing, whereas clusters characterized by concurrent reporting outages are classified as GNSS jamming.

To ensure that only statistically meaningful multi-vessel structures are interpreted as wide-area events, additional vessel-level coherence criteria are applied as part of the final categorization. Specifically, a spatiotemporal cluster is regarded as a valid multi-vessel event only when (4) it contains at least five distinct MMSIs and (5) at least 60% of the vessels within the cluster exhibit anomalous behavior. These criteria prevent clusters formed by a small number of outlier vessels embedded in otherwise normal traffic from being misinterpreted as collective anomalies. Together, they ensure that the final classification reflects a statistically coherent, region-level deviation rather than incidental or vessel-specific irregularities.

4. DATASET AND EXPERIMENTAL SETUP

4.1 AIS Dataset Specification

The AIS dataset used in this study was obtained from the national AIS archive operated by the Korea Research Institute of Ships and Ocean Engineering (KRISO). The evaluation period spans from 1 November to 30 December 2024, covering coastal and offshore waters surrounding the Korean Peninsula within latitudes 32–37° N and longitudes 123–133° E. This region encompasses major shipping lanes, port approaches, and open-sea traffic corridors, providing a representative maritime operating environment. In total, approximately 966 million AIS messages were collected during the evaluation period, representing dense vessel traffic under both coastal and offshore conditions. The large volume and high temporal resolution of the dataset enable comprehensive assessment of spatiotemporal coherence across multiple vessels, which is essential for wide-area anomaly analysis.

Each AIS message includes static identifiers, dynamic navigation parameters, and voyage-related information. A summary of the available AIS fields is provided in Table 1. Among these, only the dynamic navigation fields—timestamp, latitude, longitude, speed over ground (SOG), and course over ground (COG)—were used as inputs to the processing pipeline described in Section 3. Static and voyage-related fields were retained solely for vessel identification and data organization. A visual sample of vessel trajectories for a single day within the evaluation period is illustrated in Figure 3, highlighting the spatial density and heterogeneity of maritime traffic in the study area. All AIS messages were processed in their original temporal order without subsampling, ensuring that both short-lived and persistent anomalies could be consistently evaluated within the unified processing pipeline.

TABLE 1 AIS message fields used in the proposed framework

Category	Information	Remarks
Static Information	Ship Registration Number	Entered manually at the initial stage or when changes occur
	MMSI	
Dynamic Information	Timestamp	Automatically updated according to the vessel's navigational status
	Latitude	
	Longitude	
	Position Accuracy	
	SOG	
	COG	
	Heading	
	Rate of Turn	
Voyage-related Information	AIS Message Type	Entered manually at regular intervals
	AIS Transmit Mode	
	Base Station ID	
	Additional Navigation Data	

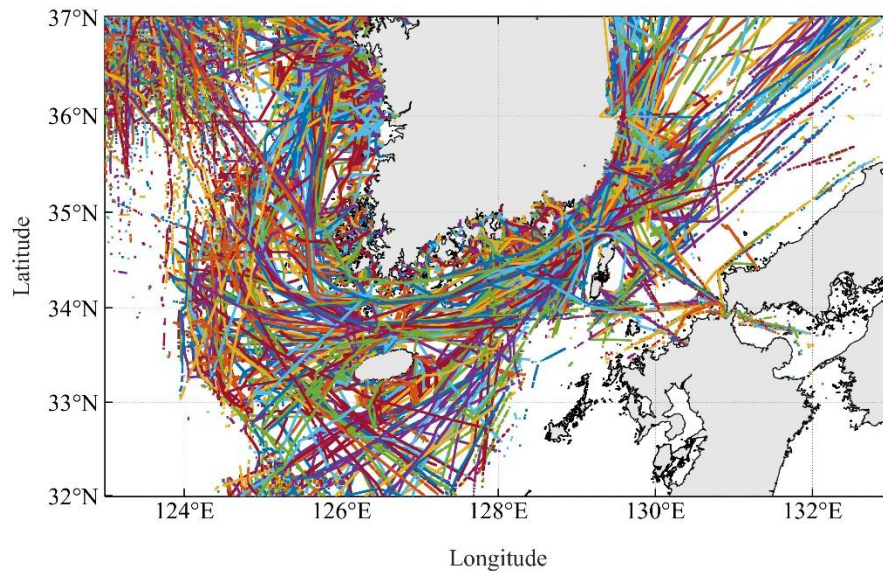


FIGURE 3 AIS vessel trajectories on 1 November 2024 within the study area (32–37° N, 123–133° E), illustrating the spatial density and heterogeneity of maritime traffic around the Korean Peninsula

4.2 Data Preprocessing

Prior to applying the processing pipeline described in Section 3, the AIS dataset was subjected to a limited set of preprocessing steps to remove obvious data redundancies and to constrain the analysis to the intended geographic scope. These steps were applied uniformly across the dataset and were designed to prepare the data for subsequent processing without introducing any anomaly interpretation or classification.

First, duplicate AIS records were removed (Ferreira et al., 2022; Tian et al., 2025). Records were considered duplicates when they contained identical MMSI identifiers, timestamps, and navigation tuples. This step addressed exact message replication arising from data aggregation or relay mechanisms and was performed solely to prevent redundant processing.

Second, AIS records exhibiting excessive spatial dispersion at identical timestamps were excluded. Specifically, when multiple position reports associated with the same MMSI and timestamp were spatially separated beyond a predefined range (116.9 m) inconsistent with vessel motion, the corresponding records were removed (Fukuda et al., 2024). This step eliminated implausible multi-position artifacts generated by synchronization or rebroadcast issues, without evaluating motion feasibility or sensor behavior.

Third, the dataset was geographically constrained by removing AIS messages located outside the vicinity of the Korean Peninsula, defined by the spatial bounds specified in Section 4.1. This filtering ensured consistency between the dataset specification and the analysis region while preventing unrelated offshore traffic from influencing the results.

No kinematic thresholds, temporal interpolation, or anomaly-specific criteria were applied during preprocessing. All remaining AIS messages were preserved in their original temporal order and passed unchanged to the subsequent processing stages. After these operations, approximately 820 million valid messages remained.

4.3 Parameter Configuration

Key parameter settings for each module are summarized in Table 2. Thresholds were selected to balance sensitivity to genuine GNSS anomalies against robustness to routine AIS variability. For spatiotemporal clustering, the spatial radius ϵ_s was set to 10 km, reflecting the typical spatial extent of local GNSS interference events in the study area, while the temporal radius ϵ_t was set to 1,800 s (30 min) so that short-term jamming episodes could be captured without merging unrelated incidents into a single event. For kinematic-consistency screening, the velocity limit $v_{\max} = 30$ m/s was adopted as a conservative upper bound that still exceeds the design speed of most merchant vessels, thereby enforcing physical realism without penalizing legitimate high-speed navigation.

TABLE 2 Parameter settings for each processing stage of the proposed framework

Stage	Parameter	Value	Reference
Preprocessing	Maximum allowable distance for position scattering ($D_{scatter}$)	116.9 m	Fukuda et al., 2024
Communication-Integrity Diagnostics	Maximum spatial separation for MMSI duplication (ϵ_{space})	3,600 m	Goodarzi & Shaabani, 2019
	Maximum temporal separation for MMSI duplication (ϵ_{time})	900 s (15 min)	Olesen et al., 2023
	Maximum allowable speed difference between consecutive reports (ϵ_{speed})	2 m/s	Data-driven
	Maximum allowable heading difference between consecutive reports ($\epsilon_{heading}$)	30°	Data-driven
Anomaly Cue Generation	Kinematic anomaly threshold based on physical speed limit (v_{th})	30 m/s	Agarwal, 2019
	Transmission-Interval anomaly threshold based on a median-gap multiplier (κ)	3.0	Data-driven
	Transmission-Interval anomaly threshold based on a minimum threshold floor (T_{min})	60 s	Data-driven
Spatiotemporal Clustering	Spatial threshold (radius) for local GNSS interference (ϵ_s)	10,000 m	Data-driven
	Temporal threshold (duration) for GNSS anomalies (ϵ_t)	1,800 s (30 min)	Data-driven
	Minimum neighboring anomalies to form a cluster (minPts)	5	Hahsler et al., 2019
	Anomalous vessel ratio threshold for Group Anomaly (Th_{group})	60 %	Data-driven
	Minimum duration for Single vessel cluster ($T_{coastal} / T_{offshore}$)	Coastal: 2 min / Offshore: 15 min	Parani, 2019

5. CASE STUDIES AND RESULTS

This section presents the results of applying the proposed hierarchical framework to the national AIS archive covering November–December 2024. Table 3 summarizes the cumulative reduction in anomaly candidates produced by each stage of the pipeline. The baseline ST-DBSCAN stage generated 3,658 kinematic anomaly candidates and 22,857 transmission-interval anomalies. During subsequent spatiotemporal density analysis, a large fraction of the cue points did not satisfy the event-formation requirement and were therefore assigned to the noise category. After integrity filtering, spatiotemporal clustering, and vessel-level coherence checks, only 17 distortion-type and 343 jamming-type events were retained—representing about 0.47% and 1.50% of the initial anomalies. The following subsections

analyze the dominant anomaly mechanisms that shaped this reduction and illustrate representative cases detected by the framework.

TABLE 3 Stage-by-stage anomaly reduction results across the proposed pipeline

Analysis Stage	Process Description	Kinematic-Consistency Cues (points / MMSIs (%))	Transmission-Continuity Cues (points / MMSIs (%))
Stage 1: Communication-Integrity Diagnostics	MMSI duplication artifacts removed	665,676 / 550 (1.03 %)	
	Stale-data retransmission artifacts removed	275 / 103 (0.19 %)	
Stage 2: Anomaly Cue Generation	Kinematic-consistency anomaly cues	81,336 / 911 (1.70%)	-
	Transmission-continuity anomaly cues for jamming	-	5,540,322 / 42,569 (79.43 %)
Stage 3: ST-DBSCAN & Final Categorization	ST-DBSCAN noise (unclustered cues)	675 / 327 (0.61 %)	114,077 / 18,067 (33.71 %)
	Persistent sensor-integrity artifacts	31,063 / 15 (0.028 %)	-
	Transient sensor-integrity artifacts	47,854 / 553 (1.03 %)	-
	GNSS spoofing	214 / 45 (0.08%)	-
	GNSS jamming	-	4,126 / 1,290 (2.41 %)
	Final multi-vessel clusters	17 clusters (0.47%)	343 clusters (1.50 %)

5.1 Communication-Integrity Diagnostics

A substantial portion of the initial anomalies originated not from GNSS degradation but from AIS communication-layer inconsistencies. These artifacts were systematically identified through the integrity diagnostics and removed before higher-level analysis. The patterns described here correspond to the largest contributors to false alarms in Table 3.

5.1.1 Concurrent MMSI Duplication

Figure 4 presents a representative case of concurrent MMSI duplication identified through the communication-integrity diagnostics. In this case, a single MMSI identifier is observed to broadcast AIS messages from spatially separated locations during overlapping time intervals. When these messages are naively reconstructed as a single vessel trajectory, the resulting track exhibits abrupt long-range position jumps that violate physical continuity constraints.

However, when the messages are examined at the sub-track level, each spatially separated segment follows a smooth and dynamically consistent trajectory. The apparent anomaly therefore does not originate from navigation sensor degradation or GNSS distortion, but from identifier-level inconsistency within the AIS communication chain. Such cases are commonly associated with reused transponders, manual configuration errors, or administrative MMSI misassignment.

The proposed communication-integrity diagnostics explicitly identify these patterns by jointly evaluating temporal overlap and spatial separation conditions, as defined in Section 3.2. Once detected, the affected records are removed prior to anomaly cue generation and spatiotemporal clustering. As reflected in Table 3, concurrent MMSI duplication accounts for a substantial portion of the initial anomaly candidates, and its early removal prevents these artifacts from propagating into subsequent kinematic or clustering-based analyses.

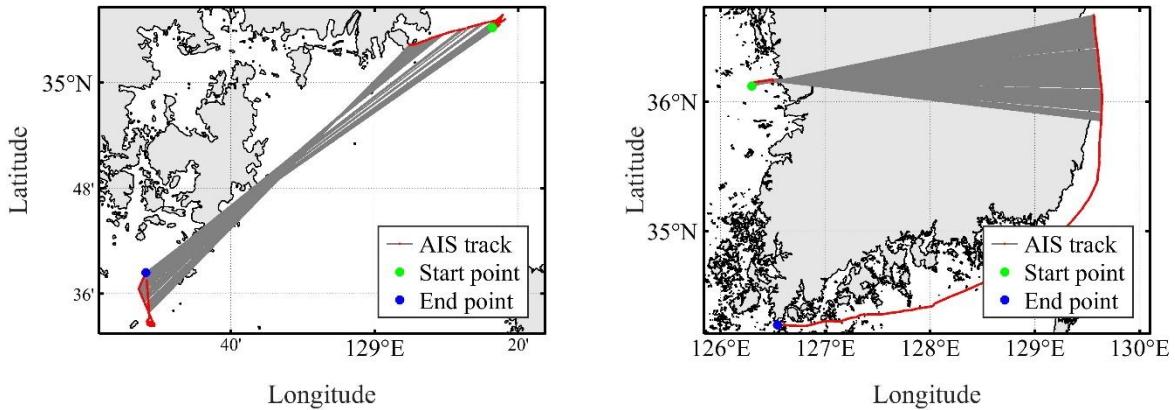


FIGURE 4 Representative case of concurrent MMSI duplication: (left) naive single-track reconstruction showing apparent long-range position jumps, and (right) sub-track decomposition revealing two spatially separated but individually consistent vessel trajectories sharing the same MMSI identifier

5.1.2 Timestamp-delayed AIS Message Retransmission

Table 4 shows a representative case of timestamp-delayed AIS message retransmission. In this example, identical navigation tuples—comprising latitude, longitude, SOG, and COG—are observed to reappear with delayed timestamps while the vessel continues normal motion. The rebroadcast messages are separated by delays on the order of tens of seconds, despite the vessel having physically progressed along its trajectory.

When interpreted without communication-integrity checks, such delayed retransmissions generate artificial trajectory artifacts, including duplicated positions, apparent backward motion, or abrupt discontinuities. Importantly, these effects arise even though the underlying navigation data themselves remain valid. The anomaly therefore reflects irregularities in message handling, buffering, or synchronization within the AIS transmission chain rather than GNSS-induced positioning errors.

The proposed diagnostics identify timestamp-delayed retransmission by detecting repeated navigation tuples with inconsistent temporal ordering, as specified in Section 3.2. Upon identification, the affected records are excluded from further analysis. This removal step is critical for preventing retransmission-induced artifacts from being misclassified as sensor-integrity anomalies or distortion-type GNSS interference during spatiotemporal clustering. As summarized in Table 4, timestamp-delayed retransmissions contribute a non-negligible fraction of communication-level anomalies and are effectively suppressed by the proposed framework.

TABLE 4 Example of timestamp-delayed AIS message retransmission

Type	Timestamp	Latitude	Longitude	SOG (m/s)	COG (°)	Elapsed Time
Original	16:55:17.570	33.046447	126.521270	7.10	196.2	-
Rebroadcast	16:56:14.590	33.046447	126.521270	7.10	196.2	+ 57.020 s

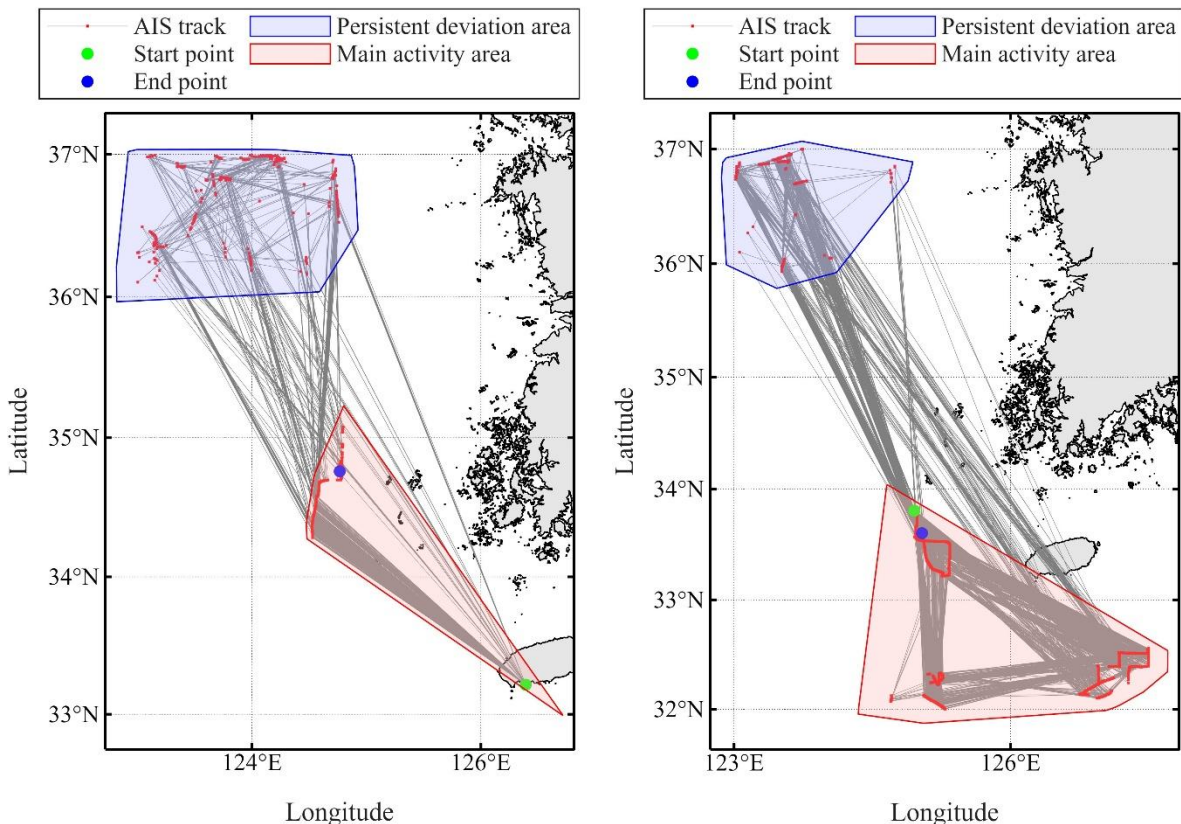
Original	16:55:47.580	33.044635	126.520480	7.25	201.5	-
Rebroadcast	16:56:34.597	33.044635	126.520480	7.25	201.5	+ 47.017 s

5.2 Sensor-integrity Artifacts

5.2.1 Persistent Sensor-integrity Artifact

Figure 5 presents representative examples of a persistent sensor-integrity artifact repeatedly observed from a single vessel throughout the entire study period. In Figure 5(a) (1 November), the vessel follows a nominal and physically plausible trajectory within its Main Activity Area, indicating normal navigation behavior. At the same time, the track exhibits recurrent, spatially detached position scatter that accumulates into a well-defined Persistent Deviation Area, forming a dense and geographically isolated footprint distinct from surrounding traffic. These deviations occur independently of the vessel's maneuvering state and local traffic conditions.

In Figure 5(b) (10 November), the same vessel demonstrates an analogous behavior on a different day, again maintaining a coherent nominal trajectory within the main operating region while producing intermittent but repeatedly occurring off-trajectory excursions within the persistent deviation footprint. Notably, this deviation pattern was observed on all 47 operational days during which the vessel reported AIS messages over the study period. The strict confinement of the anomaly to a single vessel, together with its long-term temporal persistence and the absence of contemporaneous deviations among nearby vessels, supports interpretation as a vessel-specific, persistent sensor-integrity artifact, rather than a shared GNSS interference event.



(a)

(b)

FIGURE 5 Persistent sensor-integrity artifact observed from a single vessel: (a) 1 November and (b) 10 November 2024, showing recurrent off-trajectory excursions confined to a fixed deviation area while the vessel maintains a nominal trajectory within its main activity region

5.2.2 Transient Sensor-integrity Artifact

Figure 6 presents representative examples of transient sensor-integrity artifacts that occur intermittently and remain confined to individual vessels. In Figure 6(a), the vessel exhibits oscillatory position deviations on six out of seventeen operational days during the study period. The anomaly displays a periodic structure that appears only under specific operating conditions, while the vessel otherwise follows a nominal trajectory. Such behavior is consistent with condition-dependent GNSS degradation or localized multipath effects, which can temporarily perturb position estimates without producing sustained or shared disturbances.

In Figure 6(b), a one-time parallel-track displacement is observed on a single day among sixteen operational days. The deviation is visually structured and, when viewed in isolation, may resemble short-lived spoofing at the trajectory level. However, the anomaly is strictly confined to a single vessel and does not recur in subsequent observations. Moreover, no contemporaneous deviations are observed among nearby vessels operating in the same spatial region.

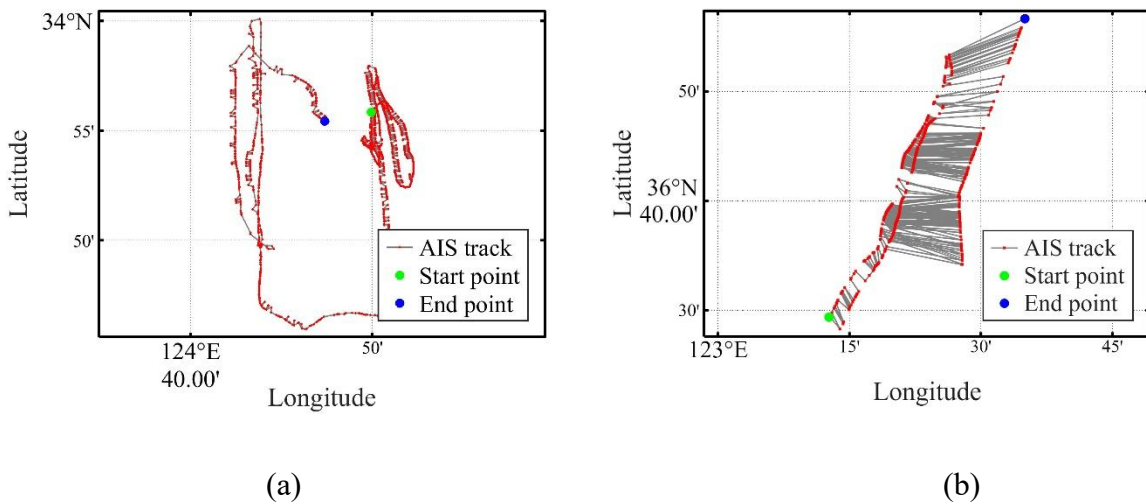


FIGURE 6 Transient sensor-integrity artifacts confined to individual vessels: (a) oscillatory position deviations appearing on 6 of 17 operational days, consistent with condition-dependent GNSS degradation, and (b) a one-time parallel-track displacement on a single day, visually resembling spoofing but absent in neighboring vessels

5.3 Spatiotemporally shared GNSS interference events

5.3.1 GNSS Spoofing

Figure 7 illustrates a representative distortion-type GNSS interference event involving multiple vessels, observed on 2 December. Figure 7(a) shows vessel trajectories extracted within a ± 10 min window centered on the event occurrence time, providing contextual information before and after the anomaly. Within this interval, multiple vessels located in close proximity exhibit pronounced position deviations, despite otherwise nominal trajectory behavior outside the event window.

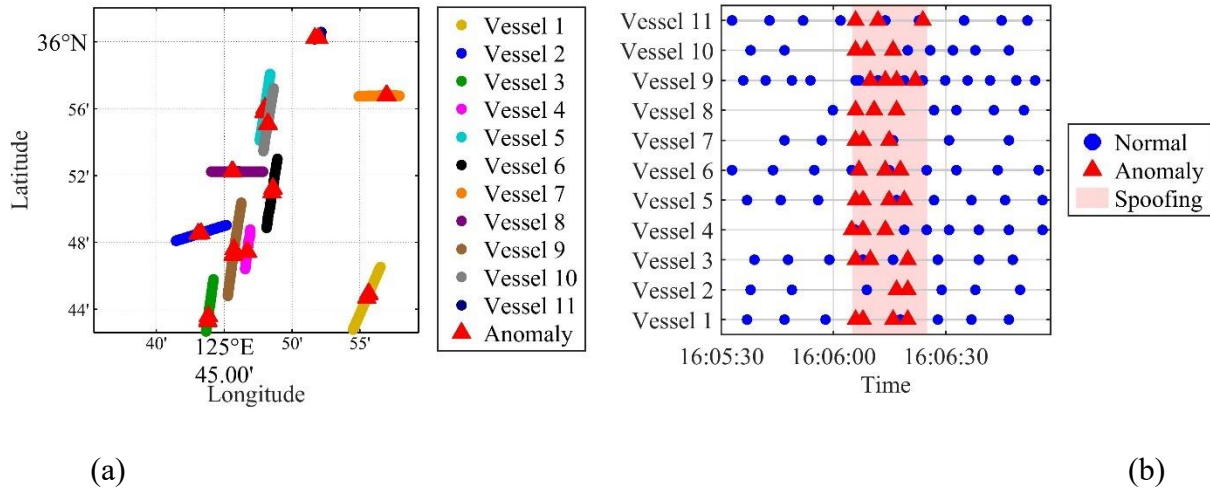


FIGURE 7 Representative GNSS spoofing event on 2 December 2024: (a) vessel trajectories within a ± 10 min window showing normal behavior outside the event, and (b) simultaneous position deviations exhibited by eleven vessels within approximately 18 km over a 20-second interval, indicating coordinated external distortion

Figure 7(b) visualizes a short temporal segment focusing on the anomaly itself. In this case, eleven vessels located within a radius of approximately 18 km simultaneously exhibited pronounced position deviations over a short interval of approximately 20 s. The anomalies emerged within the same temporal window and displayed a consistent spatial structure across all affected vessels, indicating coordinated distortion rather than independent measurement noise.

Following the removal of communication-level irregularities through communication-integrity diagnostics and the isolation of vessel-specific sensor anomalies, the remaining anomaly cues were analyzed using ST-DBSCAN. The clustering process identified the event as a dense and temporally coherent multi-vessel cluster, satisfying both the spatial proximity and temporal concurrence criteria defined in Section 3.4. The synchronized manifestation across multiple vessels operating in the same region rules out ship-specific faults and localized receiver effects.

Although the event duration is short relative to persistent sensor-integrity artifacts, the spatiotemporal coherence across multiple vessels provides strong evidence of an externally acting regional disturbance. This case highlights the effectiveness of spatiotemporal clustering in distinguishing genuine GNSS spoofing events from visually similar but vessel-confined anomalies.

5.3.2 GNSS Jamming

Figure 8 illustrates a representative wide-area GNSS jamming event characterized by synchronized signal loss across multiple vessels. In this case, eleven vessels located within a radius of approximately 21 km simultaneously experienced GNSS-related reporting outages on 9 November. Unlike distortion-type interference, the anomalies manifest as abrupt interruptions in position reporting rather than as kinematic deviations.

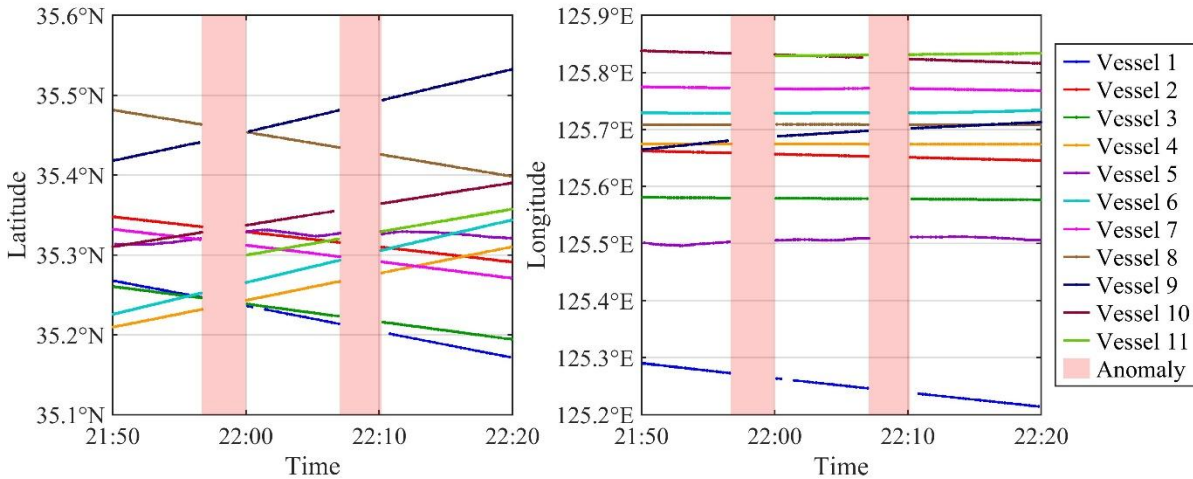


FIGURE 8 Wide-area GNSS jamming event on 9 November 2024: Time–Latitude and Time–Longitude diagrams showing synchronized reporting outages across eleven vessels within approximately 21 km, exhibiting a double-pulse temporal structure with two outage periods separated by approximately ten minutes

The Time–Latitude and Time–Longitude diagrams reveal a distinctive double-pulse temporal structure. The first outage occurred from 21:56:42 to 22:00:00, followed by a second outage from 22:07:03 to 22:10:10, with the two pulses separated by a consistent interval of approximately ten minutes. The recurrence of synchronized signal loss with a stable temporal separation across multiple vessels suggests a periodic interference mechanism rather than random receiver failure or transient environmental effects.

6. DISCUSSION

6.1 False Alarm Suppression and Classification Reliability

One of the primary challenges in AIS-based GNSS interference monitoring is the prevalence of non-interference anomalies that visually resemble spoofing or jamming. As demonstrated in Section 5, a large fraction of initial anomaly cues originate from communication-integrity issues and vessel-specific sensor faults rather than from externally induced GNSS disturbances.

The explicit separation of communication-integrity diagnostics from subsequent spatiotemporal analysis plays a critical role in suppressing such false alarms. By removing MMSI duplication and timestamp-delayed retransmissions prior to clustering, the framework prevents communication-layer artifacts from propagating into kinematic or multi-vessel analyses. This design choice is particularly important, as these

artifacts can otherwise generate dense spatiotemporal structures that are indistinguishable from genuine GNSS interference when viewed solely at the trajectory level.

Similarly, the classification of single-vessel anomalies into persistent and transient sensor-integrity artifacts ensures that vessel-specific faults are not misinterpreted as regional interference events. The results in Section 5.2 illustrate that even visually structured deviations can be reliably excluded from GNSS interference categories when temporal persistence and cross-vessel coherence are jointly considered.

6.2 Role of Spatiotemporal Coherence in GNSS Interference Identification

The case studies in Section 5.3 highlight the central role of spatiotemporal coherence in distinguishing GNSS interference from isolated positioning anomalies. Spoofing events are characterized by coordinated trajectory deviations across multiple vessels within a confined spatial region and a narrow temporal window, whereas jamming events manifest as synchronized reporting outages over broader areas.

By operating on anomaly cues rather than raw trajectories, the proposed ST-DBSCAN-based clustering framework accommodates both spoofing and jamming events within a unified analytical structure. This flexibility allows the framework to detect jamming events that would otherwise remain invisible to purely kinematic approaches, while simultaneously avoiding over-reliance on communication-layer heuristics.

6.3 Validation Challenges and Multi-Evidence Framework

A fundamental challenge in GNSS interference detection research is the scarcity of ground truth data for real-world events. Unlike controlled experiments or simulated datasets, operational maritime GNSS interference presents unique validation difficulties due to its covert nature, transient occurrence, and the absence of systematic reporting infrastructure. Deliberate jamming and spoofing are typically conducted without acknowledgment, while vessel operators may not report incidents due to operational pressures, security concerns, or lack of awareness.

This limitation is not unique to the proposed framework but represents a field-wide challenge. Among the 44 AIS anomaly detection studies surveyed by Wolsing et al. (2022), none reported validation against confirmed GNSS interference events. Recent studies have similarly relied on indirect evidence: Ferreira et al. (2022) employed domain expert review for validation, while Liang et al. (2024) used synthetic spoofing injection for testing, explicitly acknowledging the impossibility of obtaining ground truth for real-world interference.

Future validation efforts should prioritize establishing collaborative monitoring networks with maritime authorities, conducting controlled interference experiments in designated zones, and integrating AIS data with complementary sensing modalities such as ADS-B and ground-based GNSS monitoring stations. Development of standardized reporting protocols, analogous to aviation's NOTAM system, would further enable systematic ground truth collection for the maritime domain.

6.4 Operational limitations

Several inherent limitations of the proposed framework should be acknowledged. Fixed thresholds used in communication-integrity diagnostics, such as the 116.9 m criterion for position-split detection, may introduce ambiguity in boundary cases under heterogeneous network synchronization conditions. The effectiveness of kinematic anomaly cue generation further depends on onboard GNSS sensor quality, as elevated noise in aging or low-grade equipment can affect the stability of IMM-based residuals. In

addition, the framework relies on sufficient vessel density to establish spatiotemporal coherence and may exhibit reduced sensitivity to region-level GNSS interference in sparsely trafficked areas. Finally, while the classification logic distinguishes distortion-type spoofing from outage-type jamming at the phenomenological level, precise interference source localization and signal-level characterization remain beyond the scope of AIS-only analysis.

7. CONCLUSION

This study presented an AIS-based framework for identifying and classifying GNSS interference by explicitly separating communication-integrity issues, vessel-specific sensor anomalies, and spatiotemporally coherent regional disturbances. By combining rule-based diagnostics with spatiotemporal clustering of anomaly cues, the framework substantially reduces false alarms while preserving sensitivity to both distortion-type GNSS spoofing and wide-area jamming events.

Evaluation using a large-scale national AIS dataset demonstrated that the majority of apparent anomalies originate from non-interference sources, including communication artifacts and vessel-specific sensor faults. The results further showed that spatiotemporal coherence across multiple vessels provides a robust and interpretable basis for distinguishing genuine GNSS interference from visually similar but benign irregularities.

Future work will focus on extending the framework toward near-real-time monitoring, validating parameter robustness in diverse operational regions, and integrating complementary sensing modalities to support interference source characterization. The proposed approach offers a scalable and interpretable foundation for maritime GNSS interference monitoring using AIS data.

ACKNOWLEDGMENTS

This research was supported by the Regional Innovation System & Education(RISE) program through the (Chungbuk Regional Innovation System & Education Center), funded by the Ministry of Education(MOE) and the (Chungcheongbuk-do), Republic of Korea.(2025-RISE-11-014-03). This research was supported by Korea Research Institute of Ships and Ocean engineering a grant from Endowment Project of "Digital platform development to support marine digital transformation" funded by Ministry of Oceans and Fisheries. (2520000291, PES5581).

REFERENCES

- Agarwal, M. (2019, April 26). *What is the speed of a ship at sea?* Marine Insight. <https://www.marineinsight.com/guidelines/speed-of-a-ship-at-sea/>
- Androjna, A., Brcko, T., Pavic, I., & Greidanus, H. (2024). AIS data manipulation in the illicit global oil trade. *Journal of Marine Science and Engineering*, 12(1), 6. <https://doi.org/10.3390/jmse12010006>
- Birant, D., & Kut, A. (2007). ST-DBSCAN: An algorithm for clustering spatial-temporal data. *Data & Knowledge Engineering*, 60(1), 208–221. <https://doi.org/10.1016/j.datak.2006.01.013>
- d’Afflisio, E., Braca, P., & Willett, P. (2021). Malicious AIS spoofing and abnormal stealth deviations: A comprehensive statistical framework for maritime anomaly detection. *IEEE Transactions on Aerospace and Electronic Systems*, 57(4), 2456–2472. <https://doi.org/10.1109/TAES.2021.3083466>

- El Mekkaoui, S., Benabbou, L., & Berrado, A. (2022). Automatic identification system data quality: Outliers detection case. In *Proceedings of the International Conference on Industrial Engineering and Operations Management* (pp. 761–769). <https://doi.org/10.46254/AN12.20220129>
- European Union Aviation Safety Agency. (2023). *GNSS outage—Loss of GNSS signal / GPS spoofing* (Safety Information Bulletin No. 2022-02R2). https://ad.easa.europa.eu/blob/EASA_SIB_2022_02R2.pdf/SIB_2022-02R2_1
- Felux, M., Cassel, R., Becker, D., Circiu, M.-S., & Schipper, T. (2024). Observations and analysis of GNSS jamming and its impact on air navigation over Europe. *NAVIGATION: Journal of the Institute of Navigation*, 71(3), Article navi.657. <https://doi.org/10.33012/navi.657>
- Ferreira, M. D., Campbell, J. N. A., & Matwin, S. (2022). A novel machine learning approach to analyzing geospatial vessel patterns using AIS data. *GIScience & Remote Sensing*, 59(1), 1473–1490. <https://doi.org/10.1080/15481603.2022.2118437>
- Fukuda, G., Tamaru, H., Kubo, N., & Shoji, R. (2024). A study on AIS positional error analysis and transmission frequency requirements of attitude data for future vessel monitoring. *Journal of Navigation*, 77(5–6), 677–694. <https://doi.org/10.1017/S0373463325000232>
- Genovese, A. F. (2001). The interacting multiple model algorithm for accurate state estimation of maneuvering targets. *Johns Hopkins APL Technical Digest*, 22(4), 614–623.
- Goodarzi, M., & Shaabani, M. (2019). *Maritime traffic anomaly detection from spatio-temporal AIS data* (SSRN Scholarly Paper No. 3462402). Social Science Research Network. <https://papers.ssrn.com/abstract=3462402>
- Guo, S., Mou, J., Chen, L., & Chen, P. (2021). An anomaly detection method for AIS trajectory based on kinematic interpolation. *Journal of Marine Science and Engineering*, 9(6), 609. <https://doi.org/10.3390/jmse9060609>
- Hahsler, M., Piekenbrock, M., & Doran, D. (2019). dbscan: Fast density-based clustering with R. *Journal of Statistical Software*, 91(1), 1–30. <https://doi.org/10.18637/jss.v091.i01>
- Han, X., Armenakis, C., & Jadidi, M. (2021). Modeling vessel behaviours by clustering AIS data using optimized DBSCAN. *Sustainability*, 13(15), 8162. <https://doi.org/10.3390/su13158162>

Harati-Mokhtari, A., Wall, A., Brooks, P., & Wang, J. (2007). Automatic identification system (AIS): Data reliability and human error implications. *The Journal of Navigation*, 60(3), 373–389. <https://doi.org/10.1017/S0373463307004298>

International Association of Independent Tanker Owners. (2019). *Jamming and spoofing of GNSS*. INTERTANKO. <https://www.maritimelobalsecurity.org/media/1043/2019-jamming-spoofing-of-gnss.pdf>

International Association of Marine Aids to Navigation and Lighthouse Authorities. (2016). *IALA Guideline 1082: An overview of AIS*. IALA. https://www.navcen.uscg.gov/sites/default/files/pdf/IALA_Guideline_1082_An_Overview_of_AIS.pdf

International Civil Aviation Organization, International Maritime Organization, & International Telecommunication Union. (2025). *Joint statement from ICAO, IMO and ITU on interference with Global Navigation Satellite Systems*. International Civil Aviation Organization. <https://wwwcdn.imo.org/localresources/en/MediaCentre/PressBriefings/Documents/ICAO-IMO-ITU%20Joint%20Statement.pdf>

International Maritime Organization. (2002). *SOLAS chapter V, regulation 19.2: Carriage requirements for shipborne navigational systems and equipment*. International Maritime Organization. <https://www.navcen.uscg.gov/sites/default/files/pdf/AIS/SOLAS.V.19.2.1-5.pdf>

International Maritime Organization. (2021). *Deliberate interference with the United States Global Positioning System (GPS) and other Global Navigation Satellite Systems (GNSS)* [MSC.1/Circ.1644]. International Maritime Organization. https://rntfnd.org/wp-content/uploads/IMO-Circular-MSC.1-Circ.1644-Deliberate-Interference-With-The-United-States-Global-Positioning-System-Gps-And-Other...-Secretariat.pdf_safe.pdf

International Telecommunication Union. (2014). *Technical characteristics for an automatic identification system using time division multiple access in the VHF maritime mobile band* [Recommendation ITU-R M.1371-5]. International Telecommunication Union. <https://www.itu.int/rec/R-REC-M.1371-5-201402-I>

Iphar, C., Napoli, A., & Ray, C. (2020). Data integrity assessment for maritime anomaly detection. *Expert Systems with Applications*, 147, 113219. <https://doi.org/10.1016/j.eswa.2020.113219>

Last, P., Bahlke, C., Hering-Bertram, M., & Linsen, L. (2014). Comprehensive analysis of automatic identification system (AIS) data in regard to vessel movement prediction. *Journal of Navigation*, 67(5), 791–809. <https://doi.org/10.1017/S0373463314000253>

Liang, M., Weng, L., Gao, R., Li, Y., & Du, L. (2024). Unsupervised maritime anomaly detection for intelligent situational awareness using AIS data. *Knowledge-Based Systems*, 284, 111313. <https://doi.org/10.1016/j.knosys.2023.111313>

Liu, Y., Song, R., & Bucknall, R. (2019). Intelligent tracking of moving ships in constrained maritime environments using AIS. *Cybernetics and Systems*, 50(6), 539–555. <https://doi.org/10.1080/01969722.2019.1630566>

Lo, S., Liu, Z., Ibrahim, L., Chen, Y. H., & Walter, T. (2025). Observations of GNSS spoofing in Russia in 2023–2024. In *Proceedings of the ION International Technical Meeting (ITM 2025)* (pp. 425–442). Institute of Navigation. <https://doi.org/10.33012/2025.19985>

Lv, X., Jiang, R., Chang, C., Shu, N., & Wu, T. (2025). A deep learning approach for identifying intentional AIS signal tampering in maritime trajectories. *Journal of Marine Science and Engineering*, 13(4), 660. <https://doi.org/10.3390/jmse13040660>

Mai Thi, Q. A., Lee, C., Tao, T. M., & Youn, C.-H. (2024). Tracking vessel activities with AIS data using an adaptive extended Kalman filter. In *2024 15th International Conference on Information and Communication Technology Convergence (ICTC)* (pp. 349–354). IEEE. <https://doi.org/10.1109/ICTC62082.2024.10827762>

Newaliya, N., & Singh, Y. (2024). Multivariate hierarchical DBSCAN model for enhanced maritime data analytics. *Data & Knowledge Engineering*, 150, 102282. <https://doi.org/10.1016/j.datak.2024.102282>

Nguyen, D., Vadaine, R., Hajduch, G., Garelo, R., & Fablet, R. (2022). GeoTrackNet—A maritime anomaly detector using probabilistic neural network representation of AIS tracks and a contrario detection. *IEEE Transactions on Intelligent Transportation Systems*, 23(6), 5655–5667. <https://doi.org/10.1109/TITS.2021.3055614>

Olesen, K. V., Boubekki, A., Kampffmeyer, M. C., Jenssen, R., Christensen, A. N., Hørlück, S., & Clemmensen, L. H. (2023). A contextually supported abnormality detector for maritime trajectories. *Journal of Marine Science and Engineering*, 11(11), 2085. <https://doi.org/10.3390/jmse11112085>

- Parani, C. V. (2019, February 28). *Heuristics in shipboard decision-making*. SAFETY4SEA. <https://safety4sea.com/heuristics-in-shipboard-decision-making/>
- Rong, H., Teixeira, A. P., & Guedes Soares, C. (2020). Data mining approach to shipping route characterization and anomaly detection based on AIS data. *Ocean Engineering*, 198, 106936. <https://doi.org/10.1016/j.oceaneng.2020.106936>
- Siegert, G., Banyś, P., Martínez, C. S., & Heymann, F. (2016). EKF-based trajectory tracking and integrity monitoring of AIS data. In *2016 IEEE/ION Position, Location and Navigation Symposium (PLANS)* (pp. 887–897). IEEE. <https://doi.org/10.1109/PLANS.2016.7479784>
- Tian, Y., Liu, Y., Zhang, X., Yan, H., & Liu, C. (2025). Gradient-descent-based IMM smoothing for AIS trajectory reconstruction. *IEEE Transactions on Instrumentation and Measurement*, 74, Article 6511412. <https://doi.org/10.1109/TIM.2025.3617409>
- Wolsing, K., Roepert, L., Bauer, J., & Wehrle, K. (2022). Anomaly detection in maritime AIS tracks: A review of recent approaches. *Journal of Marine Science and Engineering*, 10(1), 112. <https://doi.org/10.3390/jmse10010112>
- Yang, J., Chen, B., & Ma, L. (2022). Ship trajectory tracking based on IMM-SCKF algorithm. *Chinese Journal of Ship Research*, 17(4), 12–23. <https://doi.org/10.19693/j.issn.1673-3185.02692>
- Zhang, Y., & Li, W. (2022). Dynamic maritime traffic pattern recognition with online cleaning, compression, partition, and clustering of AIS data. *Sensors*, 22(16), 6307. <https://doi.org/10.3390/s22166307>
- Zhao, L., Shi, G., & Yang, J. (2018). Ship trajectories pre-processing based on AIS data. *The Journal of Navigation*, 71(5), 1210–1230. <https://doi.org/10.1017/S0373463318000188>